# ORBITAL DYNAMICS OF HIGH AREA-TO-MASS RATIO DEBRIS AND THEIR DISTRIBUTION IN THE GEOSYNCHRONOUS REGION

**J.-C. Liou[(1)] and J.K. Weaver[(2)]**

*[(1)]ESC Group/ERC, PO Box 58447, Mail Code JE104, Houston, TX, 77258, USA,*
*Email: jer-chyi.liou1@jsc.nasa.gov*
*[(2)]NASA Johnson Space Center, 2101 NASA Parkway, Mail Code DM, Houston, TX, 77058, USA,*
*Email: jonathan.k.weaver@nasa.gov*

## ABSTRACT

A study on the orbital evolution of geosynchronous (GEO) debris with very high area-to-mass ratio (A/M) was completed recently by the NASA Orbital Debris Program Office. The objective was to find a plausible explanation for the highly eccentric GEO objects discovered by the European Space Agency's 1-m telescope and NASA's 0.6/0.9-m telescope survey. Two orbit integrators were used in the numerical simulations. Objects with A/Ms ranging from 0.1 to 35 $m^2$/kg were included. Results from the simulations indicated that solar radiation pressure could cause a high A/M debris to go through a significant yearly variation in eccentricity. The amplitude of the variation increased with increasing A/M. A group of debris with A/Ms on the order of 10 to 20 $m^2$/kg could produce observable characteristics consistent with the discovered population. We also analyzed the global behavior of thousands of high A/M debris and identified some unique patterns associated with their distribution in space. A good search strategy could be developed to maximize the detection efficiency for future GEO surveys. Finally, we considered thermal blanket pieces the most likely sources of the high A/M debris population in GEO.

## 1. INTRODUCTION

Recent observations by the European Space Agency's 1-m telescope on Tenerife (Canary Islands) have identified a new debris population near the geosynchronous orbit (GEO) region (Schildknecht et al., 2004). These faint ($18^{th}$ to $19^{th}$ magnitude), uncataloged objects have mean motions near 1 rev/day and orbital eccentricities as high as 0.55. A recent NASA GEO survey using the 0.6/0.9-m Michigan Orbital DEbris Survey Telescope (MODEST) in Chile also reveals many faint objects with high hour angle drift rates that are consistent with highly eccentric orbits (Seitzer et al., 2004). The combination of the 24-hour orbital period and high eccentricity is certainly a surprise to the orbital debris community. However, a simple explanation may solve this puzzle. These may be debris with very high area-to-mass ratios (A/Ms).

To test this high A/M hypothesis, we performed a series of numerical simulations on objects with A/Ms ranging from 0.1 $m^2$/kg to 35 $m^2$/kg using a high fidelity numerical integrator and a fast orbit propagator. Details of the numerical integrator and the orbit propagator are described in Section 2. A summary of the orbital evolution of individual debris with different A/M is also included in the section. To understand the global behavior and distribution of high A/M debris, we systematically analyzed the orbital evolution of several thousand debris released on different epochs and with different initial orbital elements. The results are described in Section 3. Seasonal variations of the high A/M debris with respect to ground-based observers, and a good search strategy to maximize detection efficiency are also presented. Possible sources of the high A/M debris are discussed in Section 4.

## 2. ORBITAL EVOLUTION OF INDIVIDUAL HIGH A/M DEBRIS

Two numerical tools were used in this study: SPCM and PROP3D. SPCM is a high fidelity orbit integrator based on Encke's method. Perturbations included in the GEO simulations were solar and lunar gravitational perturbations, geopotential Goddard Earth Model (GEM) 7x7, solar radiation pressure, Earth's shadow effects, and the reflection of solar radiation from the Earth's surface. A time step of 20 minutes was used in the integration. The reflection coefficient was set to 1.25. Output position and velocity vectors were converted to six Keplerian orbital elements in the Geocentric Equatorial Coordinate System for analysis.

PROP3D is a fast orbit propagator based on the averaging principle. Perturbations included in the GEO simulations were low-order solar and lunar gravitational perturbations, geopotential $J_2$, $J_3$, $J_4$, $(J_2)^2$, solar radiation pressure, and Earth's shadow effects. The propagation time step was set to one day in the long-term simulations. PROP3D outputs the first five Keplerian orbital elements in the Geocentric Equatorial Coordinate System. Although there were minor discrepancies between the SPCM and PROP3D results, PROP3D was able to capture the major long-term orbital characteristics predicted by SPCM. The similarity between the two model predictions indicates the orbital evolution of a high A/M object in GEO is dominated by major perturbations, not the high-order perturbations

*Proceedings of the Fourth European Conference on Space Debris, Darmstadt, Germany, 18-20 April 2005*
*(ESA SP-587, August 2005)*

ignored by the algorithm in PROP3D. SPCM was used in the analysis of the orbital evolution of individual debris. PROP3D was used in the study of groups of 1000 debris to analyze their general evolutionary characteristics and global distribution patterns.

To observe how A/M affects the orbital evolution of debris in GEO, we performed a series of numerical simulations on objects with A/Ms ranging from 0.1 $m^2$/kg to 35 $m^2$/kg. The initial mean motions, eccentricities, and inclinations were chosen from 0.998 to 1.01 rev/day, 0.001 to 0.01, and 0.1° to 1°, respectively. Two typical examples are shown in Fig. 1, where the orbital elements as functions of time are plotted. The two objects, with A/M values of 1 $m^2$/kg (left) and 20 $m^2$/kg (right), were integrated with SPCM from 1970 to 2000. Other than the A/M values, the two objects had the identical initial orbital elements. However, the difference in A/M led the two objects to two very different evolutionary paths. The former behaved just like a typical GEO object where its eccentricity remained small and its inclination varied slowly up to 15° with a period of about 52 years (observed from an extended integration). On the other hand, the orbital eccentricity of the latter went through a periodic variation with a peak value of about 0.55. The period of variation was one year. Its inclination variation was also very different from a typical GEO debris.

Analyses on other examples showed that the peak eccentricity value an object could achieve increased with its A/M. For example, the maximum eccentricities for 1, 10, 20, and 30 $m^2$/kg objects were approximately 0.03, 0.3, 0.55, and 0.7, respectively. Although their orbital periods remained close to 24 hours, their perigees could drop well below 10,000 km altitude with higher eccentricities. Regardless of the A/M values, the variations in eccentricity always maintained a one-year period.

The inclination variation of an object changed with its A/M as well. The high A/M example in Fig. 1 showed its inclination went up to about 40° with a period of approximately 16 years. Additional analyses showed that a higher A/M resulted in a higher inclination peak but with a shorter variation period. The maximum inclinations for 1, 10, 20, and 30 $m^2$/kg objects were approximately 15°, 25°, 40°, and 43°, respectively. The inclination variation periods for 1, 10, 20, and 30 $m^2$/kg objects were approximately 52, 34, 16, and 8.5 years, respectively.

The cause of the dramatic eccentricity and inclination variations is solar radiation pressure. It is well known that the perturbation causes yearly periodic variations to an object's eccentricity; and the magnitude of the variation increases with increasing A/M (*e.g.*, Vallado, 2001). These effects are well illustrated by the direct numerical integration results shown in Fig. 1. If in fact the recently discovered objects are high A/M debris, their eccentricities should go through yearly variations. GEO observers could track the same object over time, from several months up to a year, to confirm whether or not the high A/M hypothesis we propose is correct.

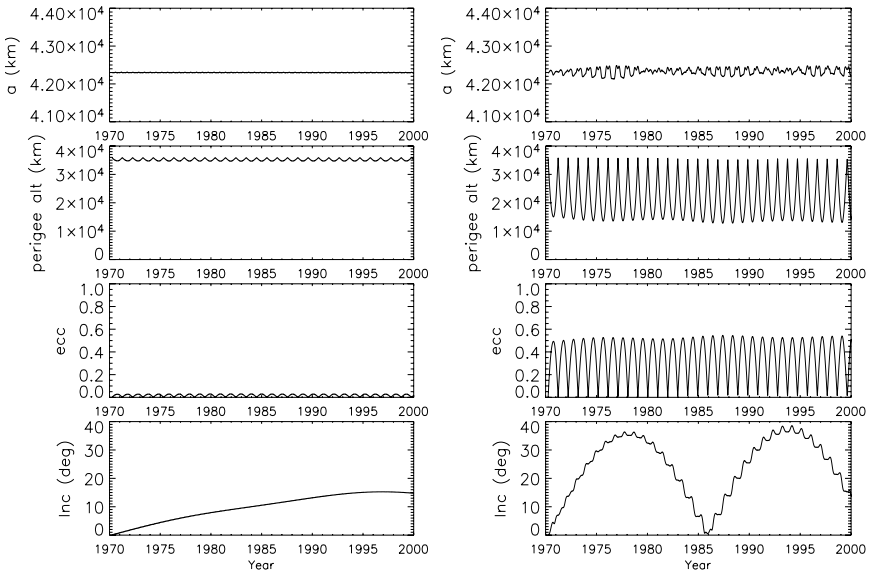


*Figure 1. Orbital histories of two GEO objects with A/Ms of 1 $m^2$/kg (left) and 20 $m^2$/kg (right), respectively. The dramatic differences between the two were caused by solar radiation pressure, the effect of which increased with increasing A/M. Note the variations might not be smooth due to the complexity of the object entering and leaving the Earth's shadow and the combination of other perturbations.*

## 3. GLOBAL BEHAVIOR OF HIGH A/M DEBRIS

To analyze the general behavior and global distribution of high A/M debris, we systematically integrated several groups of 1000 debris using PROP3D. We simulated debris released on the same epoch and with nearly identical initial orbital elements to represent population created from a single event. We also simulated debris released on different epochs and with different initial orbital elements to represent a population created from multiple events over time. Only the latter cases were summarized and described in this paper.

For the population described below, the initial release epoch and A/M for each debris were selected randomly between 1970 and 2004, and between 10 and 20 $m^2$/kg, respectively. Each object's semimajor axis ($a$), eccentricity ($e$), inclination ($i$), right ascension of the ascending node ($\Omega$), and argument of perigee ($\omega$) were also selected randomly between 42,159 and 42,259 km, between 0.0 and 0.01, between 0° and 1°, between 0° and 360°, and between 0° and 360°, respectively. All objects were propagated to a common epoch in the future, and their orbital element distributions and spatial density distributions were analyzed.

Fig. 2 shows the distributions in eccentricity and inclination of all 1000 debris on 1 January 2005. There were wide spreads in the two distributions although all objects started with very low eccentricities and inclinations. What this implies is debris with similar high A/M values, but released at different epochs, could appear, at a later point in time, as a group of objects with very different eccentricities and inclinations. When a population is observed to have wide spreads in eccentricity and inclination, it is an indication that their A/Ms could be very high, although the individual A/Ms might be very similar to one another.

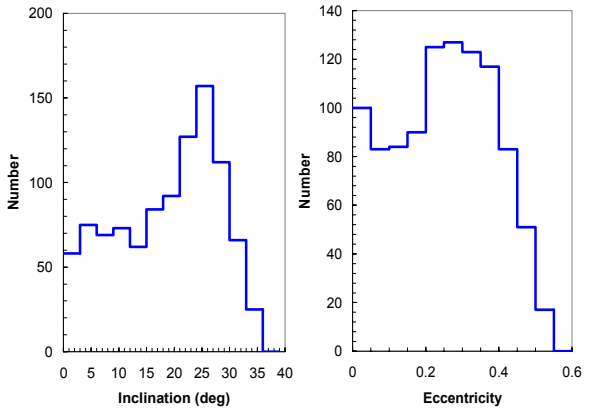


*Figure 2. Eccentricity and inclination distributions of a group of high A/M debris, on 1 January 2005, from one of the numerical simulations. These debris have similar A/M values (10 to 20 $m^2$/kg), but different release epochs.*

A different way to view the orbital element distributions is presented in Fig. 3, where the same debris from Fig. 2 are included. A new parameter, longitude of perigee, $\varpi$, is used instead of argument of perigee. It is defined as the sum of $\Omega$ and $\omega$. When the inclination is small, $\varpi$ is approximately the angular distance of perigee measured from the vernal equinox. The combinations of ($e$, $\varpi$) and ($i$, $\Omega$) are commonly used in celestial mechanics for dynamical studies (*e.g.*, Brouwer and Clemence, 1961). Patterns in ($e$, $\varpi$) and ($i$, $\Omega$) indicate non-uniform distribution in space.

Two prominent features can be observed from Fig. 3. First, all points are nicely confined to a ring-like structure in ($i\cdot\cos\Omega$, $i\cdot\sin\Omega$) space, with the center of the ring approximately 14° separated from the origin (lower-right panel). A direct consequence of this distribution is the plane of symmetry, which for debris with A/Ms between 10 and 20 $m^2$/kg, is tilted approximately 14° with respect to the equatorial plane. The ascending node of this plane points very close to the vernal equinox. The radius of the ring is about 23°. As each debris evolves with time, its corresponding point in Fig. 3 moves along the ring in a clockwise direction over a period of 16 to 34 years (depending on A/M). The size and location of the ring vary with the A/M distribution of the population. Higher A/Ms increase the radius of the ring while keeping the left end of the ring close to the origin. The difference between 10 and 20 $m^2$/kg for this set of simulations leads to the wide spread in the right half of the ring.

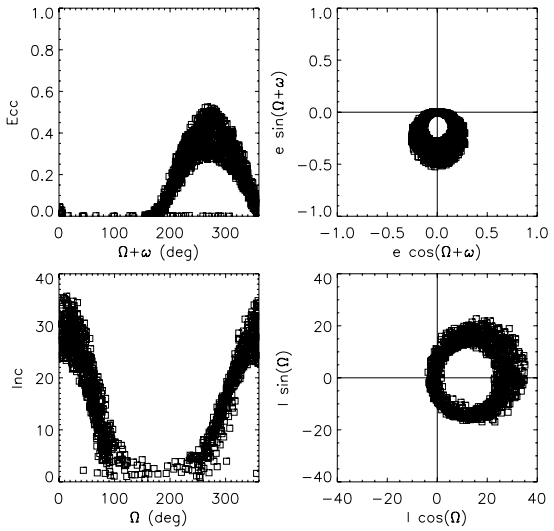


*Figure 3. Orbital element distributions for a group of 1000 high A/M debris in 2005. The evolutions of high A/M debris follow distinct patterns in (e, Ω+ω) and (I, Ω). The ring-like structures in the two right panels have special dynamical meanings, and lead to some interesting geometric patterns for their distributions in space.*

The second interesting feature in Fig. 3 (upper right panel) is the ring-like structure in ($e\cdot\cos\varpi$, $e\cdot\sin\varpi$). Although similar to that in ($i\cdot\cos\Omega$, $i\cdot\sin\Omega$) space, it has a different geometrical meaning. As each debris evolves with time, its corresponding point on the ($e\cdot\cos\varpi$, $e\cdot\sin\varpi$) plot moves, counter-clockwise, along the ring with a period of one year. Additional analyses indicate this annual motion is related to the position of the Sun. In other words, the perigees of high A/M debris tend to line up toward the Sun, and they move accordingly over the course of one year. For GEO surveys where search areas typically follow the anti-Sun direction, high A/M debris are likely to be detected near apogees where their hour angle drift rates are slower than typical circular GEO debris.

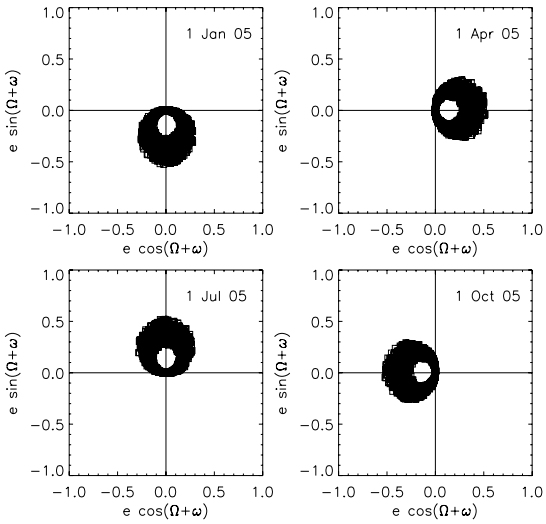


*Figure 4. The distribution in ($e\cdot\cos\varpi$, $e\cdot\sin\varpi$) changes over the course of one year. The perigees of the high A/M debris tend to line up toward the Sun.*

The ring-like structure in ($e\cdot\cos\varpi$, $e\cdot\sin\varpi$) changes rapidly during the course of one year while the pattern in ($i\cdot\cos\Omega$, $i\cdot\sin\Omega$) remains almost unchanged during the same period. The combination of these features and the geometries mentioned above lead to some unusual distributions in space that can be utilized to aid future GEO surveys. Fig. 4 shows the ($e\cdot\cos\varpi$, $e\cdot\sin\varpi$) distributions at four snapshots in 2005. In late March (upper right panel), the Sun is near vernal equinox and the anti-Sun direction is 180° away pointing toward the descending node where the plane of symmetry intersects the equatorial plane. The distribution in ($i\cdot\cos\Omega$, $i\cdot\sin\Omega$) indicates an anti-solar-direction survey could concentrate near the equator. High A/M debris would be near their descending nodes and should have high negative (southward) declination drift rates. The distribution in ($e\cdot\cos\varpi$, $e\cdot\sin\varpi$) indicates the same anti-solar-direction survey near the equator would see the same A/M debris near their apogees (upper right panel). Their right ascension drift rates should be slower than those expected from the typical near-circular GEO objects.

The search strategy is different three months later (1 July 2005) when the Sun is 90° ahead of the vernal equinox. The distribution in ($i\cdot\cos\Omega$, $i\cdot\sin\Omega$) indicates an anti-solar-direction survey should not concentrate near equator. The plane of symmetry for high A/M debris (10 to 20 $m^2$/kg) is about 14° below the equator along the anti-Sun direction. High A/M debris would be near the southern-most parts of their orbits and should have nearly zero declination drift rates. The distribution in ($e\cdot\cos\varpi$, $e\cdot\sin\varpi$) again indicates the same anti-solar-direction survey would see high A/M debris near their apogees (lower left panel). Their right ascension drift rates should be slower than those expected from the typical near-circular GEO objects. Fig. 5 provides a simple illustration for the above-mentioned geometry.

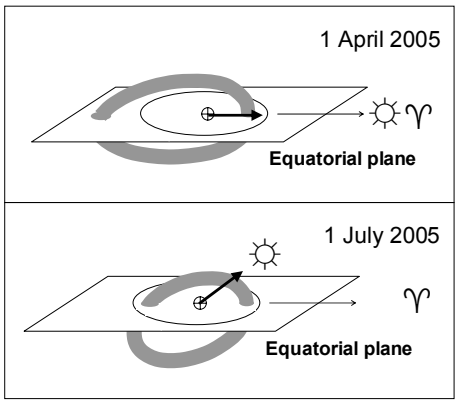


*Figure 5. A simple illustration of the distribution of high A/M debris near GEO. The epochs for the top and bottom panels are 1 April 2005 and 1 July 2005, respectively. The plane of the ring, representing the plane of symmetry for debris with A/Ms between 10 and 20 $m^2$/kg, is tilted about 14° with respect to the equatorial plane. Light arrows point to vernal equinox (indicated by ♈) while bold arrows indicate where the perigees are. In general, the perigees of high A/M debris are concentrated toward the Sun (indicated by ☼). The circle on the equatorial plane represents the orbit of a circular GEO object.*

The faint objects with high hour angle rates identified in the NASA MODEST GEO survey are consistent with high A/M debris. Fig. 6 is adopted from the NASA Orbital Debris Quarterly News Vol. 8, Issue 1 (Seitzer et al., 2004). It shows the angular rates of the 510 uncataloged objects observed by MODEST between November 2002 and April 2003. The bright and faint debris have very different distributions in hour angle rate.

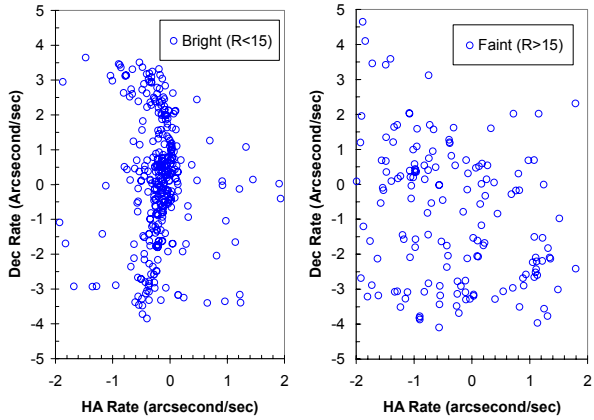


*Figure 6. The observed hour angle (HA) rates versus declination (Dec) rates of 510 uncataloged objects in GEO. The data were taken by MODEST between 11/2002 and 04/2003 (Seitzer et al., 2004).*

Fig. 7 shows hour angle rates versus declination rates for two simulated GEO populations. Each population consists of 1000 debris released between 1970 and 2004, and propagated to 2005. The A/Ms of the population in the left panel are all below 0.1 $m^2$/kg. The A/Ms of the population in the right panel range from 10 to 20 $m^2$/kg. The wide spread in hour angle draft rate for the high A/M population is very similar to that of the faint debris in the MODEST survey (right panel in Fig. 6).

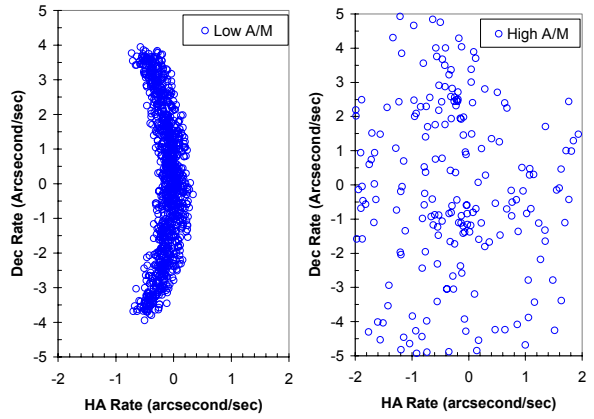


*Figure 7. Hour angle (HA) rates versus Declination (Dec) rates for two simulated GEO populations. The A/Ms of the population to the left are all below 0.1 $m^2$/kg while the A/Ms of the population to the right range from 10 to 20 $m^2$/kg. The wide spread in HA rate is the consequence of high eccentricities. Note there are additional points outside the HA and Dec ranges in the right panel.*

## 4. POSSIBLE SOURCES OF HIGH A/M DEBRIS

Is it possible to have a population of debris with A/M as high as 20 $m^2$/kg that would match the maximum eccentricity of 0.55 or even higher? Some surfaces of spacecraft and upper stages are covered with thermal blankets, or Multi-Layer Insulation (MLI). MLI often consists of layers of dacron nettings and thin aluminized Mylar®, Kapton®, or Nomex®. Typical areal density will give the corresponding A/Ms of the thin aluminized layers varying from below 10 $m^2$/kg to more than 20 $m^2$/kg. The high A/M debris detected in GEO by ESA and NASA might be MLI pieces on the order of tens of centimeters across.

There are two possible mechanisms to generate MLI pieces. The first one is the breakup of satellites or upper stages. For example, analyses of Nimbus and Ariane explosions indicated that some of the detected debris might be high A/M MLI pieces (*e.g.*, Johnson, 1989; Nauer and Johnson, 1991; Jehn, 1994). The second mechanism is satellite or upper stage surface degradation due to impacts by small meteoroids or orbital debris. There are well documented cases of MLI pieces coming off active satellites in low Earth orbit - Hubble Space Telescope (Bretz et al., 2004), Far Ultra-violet Spectroscopic Explorer (FUSE Satellite Released Unexpected Debris, 2005); and in interplanetary space - Solar Heliospheric Observatory (ESA/SOHO, 2005). Both mechanisms could lead to the build up of an MLI fragment population in GEO over time. This might be the population that was recently discovered by ESA and NASA. Future spectroscopic observations, with improved capability of tracking faint objects in GEO, should be able to verify whether or not these objects are indeed MLI pieces.

The existence of a highly eccentric GEO population may have important implications for the environment. Although they spend less time in the GEO traffic zone (35,286 to 36,086 km altitude), their encounter speed with a GEO operational satellite should be higher than that between two typical GEO objects. They could also interfere with spacecraft at other altitudes, including Global Positioning System (GPS), GLONASS, and Galileo. Whether or not this population poses significant collision risks to operational satellites in GEO and other important altitudes needs to be modeled carefully.

**Acknowledgement**

The authors would like to thank K. Abercomby for insightful comments and suggestions on MLIs, and S. Portman for providing editorial support for the manuscript.

## 5. REFERENCES

Bretz, D.R. et al., *Photographic Survey of the Hubble Space Telescope Multi-Layer Insulation During Servicing Mission 3B*, JSC-62523, 2004.

Brouwer, D. and Clemence, G., *Celestial Mechanics*, Academic Press, Orlando, Florida, 1961.

FUSE Satellite Released Unexpected Debris, Orbital Debris Quarterly News, Vol 8, Issue 3, NASA Johnson Space Center, 2005.

Jehn, R., Analyzing and modeling Debris in the Geostationary Transfer Orbit, Space Control Conference, 1994.

Johnson, N.L., Preliminary Analysis of the Fragmentation of the Spot 1 Ariane Third Stage, in *Orbital Debris from Upper-Stage Breakup* (J.P. Loftus Jr., Ed), Progress in Astronautics and Aeronautics Vol. 121, AIAA, 1989.

Nauer, D.J. and Johnson, N.L., The Fragmentation of the Nimbus 6 Rocket Body, Teledyne Brown Engineering Technical Report CS91-TR-JSC-017, 1991.

Schildknecht, T. et al., Optical Observations of Space Debris in Highly Eccentric Orbits, 2004 COSPAR, in press.

Seitzer, P. et al., Results from the GEO Debris Survey with MODEST, Orbital Debris Quarterly News, Vol 8, Issue 1, NASA Johnson Space Center, 2004.

Vallado, D.A., *Fundamentals of Astrodynamics and Applications*, 2nd Ed, Kluwer Academic, 2001.